Human blastoid from primed human embryonic stem cells

Satoshi Imamura[1]†, Xiaopeng Wen[1]†, Shiho Terada[1], Akihisa Yamamoto[2], Kaori Mutsuda-Zapater[1,3], Kyoko Sawada[1,4], Koki Yoshimoto[1,5,6], Motomu Tanaka[2,7], and Ken-ichiro Kamei[1,8,9]*

Affiliations:

[1]Institute for Integrated Cell-Material Sciences (WPI-iCeMS), Institute for Advanced Study, Kyoto University; Yoshida-Ushinomiya-cho, Sakyo-ku, Kyoto, 606-8501, Japan

[2]Center for Integrative Medicine and Physics, Institute for Advanced Study, Kyoto University; Yoshida-Ushinomiya-cho, Sakyo-ku, Kyoto, 606-8501, Japan

[3]Graduate School of Advanced Integrated Studies in Human Survivability, Kyoto University; 1 Nakaadachi-cho, Yoshida, Sakyo-ku, Kyoto 606-8306, JAPAN

[4]Faculty of Pharmaceutical Sciences, Kyoto University; Yoshida-Ushinomiya-cho, Sakyo-ku, Kyoto, 606-8501, Japan

[5]Laboratory of Cellular and Molecular Biomechanics, Graduate School of Biostudies, Kyoto University; 53 Kawahara-cho, Shogoin, Sakyo-ku, Kyoto, 606-8507, Japan

[6]Department of Biosystems Science, Institute for Life and Medical Sciences, Kyoto University; 53 Kawahara-cho, Shogoin, Sakyo-ku, Kyoto, 606-8507, Japan

[7]Physical Chemistry of Biosystems, Institute of Physical Chemistry, University of Heidelberg, 69120, Heidelberg, Germany

[8]Department of Pharmaceutics, Wuya College of Innovation, Shenyang Pharmaceutical University; Shenyang, Liaoning 110016, PR China

[9]Department of Pharmaceutics, School of Pharmacy, Shenyang Pharmaceutical University; Shenyang, Liaoning 110016, PR China

*Corresponding author. Email: kamei.kenichiro.7r@kyoto-u.ac.jp

†These authors contributed equally to this work.

Abstract: Artificial human blastoids investigate fundamentals of early embryo development using *in vitro* models and study the pregnancy failures and birth deficiencies, previously hindered by the need for human embryos. Recent methods on generating blastoids used human naive pluripotent stem cells, which are prone to genomic instability during *in vitro* culturing. We introduce a simple, robust, and scalable method for generating human blastoids from more stable, human-primed, embryonic stem cells (hESC). Using a non-cell-adhesive hydrogel, hESC aggregates received the chemophysical cellular environment and formed an asymmetric blastoid structure with a cellular distribution similar to that of a human blastocyst. The obtained blastoids also demonstrated the capability of implantation *in vitro*. This model will allow studies on the underlying mechanisms of human pre- and post-implantation processes, leading to assisted reproductive technology.

One-Sentence Summary: Blastoids were generated from human-primed embryonic stem cells using appropriate chemophysical extracellular environments.

Main Text: A blastocyst is a cell aggregate with a cyst developed from the fertilized egg of a mammal, approximately 5 to 8 days after fertilization. It consists of epiblast (EPI), trophectoderm (TE), and primitive endoderm (PE) lineages. After blastocyst implantation, the TE and PE lineages give rise to the placenta and yolk sac, respectively (*1*). Conversely, the EPI lineage will form all three germ layers (e.g., ectoderm, mesoderm, and endoderm) that differentiate most types of tissue cells in the body (*2*) , germ cells, and embryonic stem cells (ESCs). This structure, with its unique cell positioning, is essential for further embryonic development, tissue-specific lineage cell differentiation, and organ and body structure formation. The potential uses of blastocysts are fourfold. They can 1) aid the study of the early cell development, 2) be used in drug discovery for pregnancy failure (e.g., repeated implantation failure (*3*)), 3) be used to prevent birth deficiencies (*4*) and 4) be used for the advancement of assisted reproduction technology (*5*).

Unfortunately, it is difficult to obtain blastocysts from fertilized eggs for fundamental research. Moreover, using blastocysts at the industrial level is hampered by limited cell sources, donors, and ethical concerns. Pluripotent stem cells, however, have great potential for applications in regenerative medicine and drug discovery. These cells include ESCs (*2*) and induced pluripotent stem cells (iPSCs) (*6*, *7*). They also serve as a cell source for studying the pluripotency of stem cells *in vitro* (*8*, *9*). However, the other processes of human embryonic development (e.g., blastocyst development and the implantation process) are largely unknown, compared to experimental animals (e.g., mice). This is due to a lack of *in vitro* research tools, limited *in vivo* access, and ethical issues. Recent studies have reported methods called “blastoids” to generate blastocyst-like structures in mouse models (*10–12*). Recently, three groups reported the generation of human blastoids (*13–16*). Liu et al. (2021) used cells during the reprogramming process from fibroblasts to human pluripotent stem cells (hPSCs), as these cells contained a variety of cells, including cells with EPI-, TE-, and PE-like transcriptional signatures (*13*). Yu et al. (2021) (*14*) and Yanagida et al. (2021) (*15*), however, used naïve hPSCs to generate blastoids, since recent studies have shown that naïve hPSCs can differentiate into EPI-, TE-, and PE-like cells. However, naïve hPSCs show genomic instability during culturing because of the hypomethylated state of the genome (*17*, *18*). The culturing conditions for naïve hPSCs are still being optimized, compared to those of primed hPSCs. Since most commonly used hPSCs show primed states, it would be beneficial to use primed hPSCs to generate blastoids.

To generate blastoids, we focused on the physical environment surrounding natural human blastocysts. We found that human blastocysts were surrounded by a zona pellucida (ZP) glycoprotein layer, which provides a unique physical environment with 3.39 ± 1.86 kPa of Young’s modulus (*19*). Moreover, it has been shown that primed hPSCs convert to the naïve-like state when three-dimensional (3D) culturing is applied (*20*). Therefore, we used a hydrogel (HG) that allows tuning of the extracellular environmental properties to mimic the zona pellucida layer and convert the primed hPSCs to the naive state, leading to blastoid generation. Moreover, we also hypothesized that the asymmetric structure of blastocysts could be generated by local concentration gradients of growth factors and cytokines; thus, the HG would be suitable for generating such gradients.

Here, we developed a method to generate blastoids, namely HG blastoids (HG-blastoids), from primed hPSCs in a HG medium through 3D cell culturing. This method uses a thermo-responsive HG (a copolymer of poly(*N*-isopropyl acrylamide) and poly(ethylene glycol) (PNIPAAm-PEG)) (*21*, *22*), which holds hPSC aggregates with the stimulation of elastic force against the growth thereof, without adhering to the cells. Additionally, because it can perform a sol-gel transition

via temperature change, the HG allows the mixing and harvesting of cell aggregates from the solution at a low temperature (<20 °C). Furthermore, 3D cell culturing in the HG-containing medium can be performed at 37 °C. Since serum contains a variety of growth factors for inducing differentiation of hPSCs to trophoblasts (*23*) and maintaining hPSC self-renewal, it would allow for the generation of asymmetric blastocyst-like cysts. After generating HG-blastoids, we conducted a variety of assays to determine the cellular identities and their locations within the HG-blastoids and investigated their functionalities, such as derivation of pluripotent/trophoblast stem cells and implantation, as an *in vitro* model of a human blastocyst.

Generating human blastoids in hydrogel

To generate human HG-blastoids from primed hPSCs, we created a physical environment using a HG, to mimic a ZP glycoprotein layer (**Fig. 1A**). We used KhES1 hESCs expressing an EPI marker fused to the enhanced green fluorescent protein (eGFP), downstream of the octamer-binding transcription factor 4 promoter (OCT4; or POU domain, class 5, transcription factor 1 [POU5F1]), to visualize cells expressing OCT4 and ICM-like cell aggregates in blastoids. The EPI marker used was called K1-OCT4-eGFP (*24*). We used the mTeSR-1 medium to maintain primed hPSCs (*25*, *26*). In terms of the HG, we found that 10 % (v/v) of PNIPAAm-PEG (HG), which provides 0.15 ± 0.04 kPa of Young's modulus, allows culturing of primed hPSCs (*21*) (**fig. S1 and table S1**); hence, we used this HG for blastoid generation.

To obtain hPSC aggregates of uniform size (and to increase reproducibility), single-cell-dissociated primed hPSCs cultured in a 2D-culture dish were transferred to an AggreWell plate (*27*, *28*) and cultured in mTeSR-1 medium supplemented with 10 μM Y27632 ROCK inhibitor (*29*) for 1 day. Next, K1-OCT4-eGFP aggregates were harvested from the AggreWell plate, placed in DMEM supplemented with 10 % (v/v) HG solution at 4 °C, and transferred to an ultralow attachment cell-culture dish at 37 °C. Next, DMEM supplemented with 10 % (v/v) FBS was added to create a gel condition. After 3 days of culturing, the culture medium got replaced with iBlastoid medium (*13*) and cultured for a further 6 days to form HG-blastoids.

Of the 454 hPSC aggregates cultured in the HG mixed with DMEM/FBS, 64 (14.1 %) formed a blastocyst-like structure (**Fig. 1B**). A small portion of the cell aggregates expressed the *OCT4* promoter-driven eGFP, representing the ICM-like structure. However, the outer cell layer did not adequately express eGFP (**Fig. 1C**). These results suggest that HG conditions with serum induced the differentiation of cells at the outer layer of cell aggregates, whereas the cells inside the aggregates maintained *OCT4* expression. To confirm the cellular distribution representing a human blastocyst in HG blastoids, we observed the expression patterns of typical markers, including OCT4 (epiblast), CDX2 (trophectoderm), and SOX17 (primitive endoderm) (**Fig. 1D and fig. S2**). These results indicated that the obtained HG-blastoids mimicked the cellular distribution of the three lineages in the natural blastocyst.

Single-cell transcriptomics of human HG-blastoids

To investigate cellular identities in HG-blastoids, single-cell RNA sequencing (scRNA-seq) (*30*, *31*) was performed using approximately 400 HG-blastoids containing 5,559 cells (**Fig. 2A**). We showed that HG-blastoids had three lineages, as identified by their corresponding gene markers (*POU5F1, NANOG*, *SOX2,* and *NODAL* for EPI cells; *GATA2*, *GATA3,* and *ABCG2* for TE cells; *GATA6*, *FN1,* and *COL4A1* for PE cells; **Fig. 2B, C and fig. S3**). By comparing the

scRNA-seq data with that of the original hESCs (13,516 cells), using unsupervised clustering, we observed that some clusters overlapped between hESCs and HG-blastoids (**fig. S4**). Although hESCs have two major cell populations, they strongly express *POU5F1*. Compared with hESC transcriptomic signatures, a cluster shown in light blue in **Fig. 2A** was observed only in HG-blastoids, unlike hESCs, which showed TE- and PE-like transcriptomic patterns. Similar to **Fig. 2A**, we also found some extracellular populations, which could not be assigned to EPI-, TE- or PE-like cells, and thus were named "Intermediated (IM)" cells.

Next, we used comparative transcriptomics to determine whether the EPI-, TE- and PE-like cells in HG-blastoids showed similarities in transcription signatures to natural human blastocysts. Here, scRNA-seq data of human blastocysts on days 5 to 7 (E5-7) (Petropoulos et al. (*32*)) were compared to our data (**Fig. 2D,** and **fig. S5**). Considering the integrated UMAP, HG-blastoids had EPI- (Clusters #3, #8, and #10), TE- (Clusters #1 and #2), and PE-like cells (Cluster #5) assigned to E5-7 cellular populations by their transcriptomic signatures. Next, an enrichment analysis of gene ontology (GO) terms was performed for each cluster (**figs. S6** and **S7**). EPI-like clusters had "signaling pathways regulating pluripotency of stem cells (ko04550)," "embryonic morphogenesis (GO:0048598)," and "cell division (GO:0051301)," which are important functions of EPI. In TE-like clusters, the GO term of "placenta development (GO:0001890)" was significantly enriched, indicating the potential of TE differentiation to the placenta, which is a critical process of blastocyst implantation. PE-like clusters showed an enrichment in "endoderm formation (GO:0001706)," indicating PE formation.

Although a similar percentage of cells was observed in both HG-blastoids and E5-7 blastocysts, HG-blastoids showed fewer populations of TE- and PE-like cells (**fig. S8**). More specifically, E5-7 blastocysts had 24.2 %, 65.2 %, and 20.5 %, of EPI-, TE-, and PE-like cellular populations, respectively, while HG-blastoids had 21.4 %, 27. 9%, and 1.08 %. However, HG-blastoids had additional cellular populations. For example, cells in cluster #0 were present in both human blastocysts and HG-blastoids, although to a lesser degree in human blastocysts, 4.69 % vs. 34.0 % in HG-blastoids (**fig. S8**). According to the GO enrichment analysis, "appendage development (GO:0048736)" and "cell division (GO:0051301)" were highlighted in HG Blaastoids. With regard to cluster #9, the GO term "Extracellular matrix organization (R-HAS-1474244)" was enriched. Because HG physical stimuli were introduced to generate HG-blastoids, cells might be involved in the process of ECM (extracellular matrix) remodeling. These results suggest two possible future directions. One is to improve the efficacy of direct differentiation of the TE and PE lineages with both chemical and physical stimuli, while the second is to collect blastoids. It is important to note that we collected HG-blastoids by evaluating their microscopic morphologies, without analyzing their molecular signatures. This may cause contamination with other cell aggregates with partial induction toward blastoid generation, resulting in single-cell profiles. Thus, the development of HG-blastoids similar to natural human blastocysts needs further improvement.

Finally, we the transcriptomic signatures of individual cells in HG-blastoids with those published by three other groups in 2021. These groups reported the generation of blastoids *in vitro* (*13–15*). By integrating our scRNA-seq data sets with theirs, along with data from human E5–E7 blastocysts (*32*), we investigated the differences and advantages over the other methods (**Fig. 2D and E**). UMAP integration of these datasets revealed that all methods provided blastoids with EPI-, TE-, and PE-like clusters; however, the cellular populations were quite different (**fig. S8**). Although the number of cells (306) in the dataset of Yanagida et al. (2021) was much smaller than the rest (Yu et al., 2021 [6,840 cells]; Liu et al., 2021 [7,778 cells]; our data [5,559 cells]),

Yanagida's blastoids had cells assigned to EPI, TE, and PE clusters. Moreover, their blastoids showed close similarity to the cellular profiles of human E5-7 blastocysts. Conversely, blastoids generated by Liu et al. (*13*) and Yu et al. (*15*) showed more heterogeneous populations, wherein E5-7 blastocysts were absent. Moreover, a key difference was found in cluster #11. This cluster was absent in HG-blastoids and E5-E7 blastocysts but present in the other blastoids, ranging from 1 % to 9 % of cells. Furthermore, cluster #11 showed apoptotic cells with enriched GO terms related to apoptosis (e.g., "apoptotic signaling pathway [GO:0097190]" and "positive regulation of cell death [GO:0010942]"), suggesting that their method may cause cellular damage during blastoid formation. Our method, however, with the use of HG, provides more suitable conditions without harmful cell damage.

Deriving naive/primed PSCs and TSCs from HG-blastoids

Natural blastocysts provide pluripotent and trophoblast stem cells (PSCs (*2*) and TSCs (*33*), respectively). To evaluate whether the generated HG-blastoids could generate these stem cells, we digested the HG-blastoids and cultivated the cells under the culture conditions for naive/primed PSCs and TSCs, namely naive/primed bPSCs and bTSCs, respectively (**Fig. 3A**). The obtained naive bPSCs showed a typical semi-spherical colony morphology and expressed KLF4, NANOG, and OCT4 (34) (**Fig. 3B and fig. S9A**). The obtained primed bPSCs showed a flat colony morphology and expressed TRA-1-60, OCT4, and NANOG (**Fig. 3C and fig. S9B**). The original hESCs used in this study were maintained in a primed PSC culture medium, mTeSR-1 (26); however, the obtained HG-blastoids showed the capability of providing all three stem cells, suggesting that our method to generate blastoids is also a new method to obtain naive bPSCs from primed hPSCs. While maintaining TSCs (33), bTSCs expressed KRT7, CDX2, and GATA2, markers associated with TSCs (*33*) (**Fig. 3D and fig. S9C**). Thus, we conclude that the HG-blastoid has a set of stem cell lineages that a natural human blastocyst has.

In vitro implantation assay for human HG-blastoids

In the human implantation process, trophoblasts of a blastocyst attach to the uterine wall, and 4 days after adhesion, the inner cell mass turns to the pro-amniotic cavity and epiblasts. To evaluate whether human HG-blastoids showed such blastocyst functionality, HG-blastoids were transferred onto the cell-culture dish coated with GelTrex extracellular matrices to recapitulate the implantation process *in vitro* (**Fig. 4A**). After attachment, the HG-blastoids gradually expanded and grew on the substrate (**Fig. 4B**).

In light of previous reports, an *in vitro* implantation assay for a human blastocyst is capable of recapitulating the formation of a lumen like a pro-amniotic cavity (*35*, *36*). The attached HG-blastoids formed a pro-amniotic-like cavity, in which F-actin and aPKC were expressed in the lumen region, while OCT4-positive EPI-like cells were expressed around the lumen, as confirmed by immunocytochemistry (**Fig. 4C**). Moreover, co-staining experiments using OCT4 (EPI), KRT7 (TE), and SOX17 (PE), revealed that OCT4-positive cells showed cell aggregates with high cellular densities, a feature of EPI. Furthermore, SOX17-positive PE-like cells were located on the side of EPI-like cell aggregates, while KRT7-positive TE-like cells showed outgrowths from the attached areas (**Fig. 4D**). As shown in **Fig. 4E**, the cells expressing the GATA6 PE marker were next to the NANOG-positive EPI-like cell aggregates, a feature of PE-like cells. These results were in agreement with the staining results shown in **Fig. 4D**.

To evaluate TE-like features in detail, MMP2 and hCG were stained as representative markers of extravillous cytotrophoblasts (EVTs) and syncytiotrophoblasts (STs), respectively (**Fig. 4F and G**). Close observation of hCG-positive ST-like cells and their nuclei, showed some cells with multiple nuclei, representing a unique feature of ST-like cells (37) (**Fig. 4G**). Conversely, MMP2 positive cells showed spindle-like morphologies, a cellular phenotype of EVT-like cells (*37*). Next, RT-PCR was used to quantify the expression of genes associated with EVT- and ST-like cells. All of the EVT marker genes (e.g., *ITGA1*, *ITGA5*, and *FN1*) were highly induced after attachment, while only the *hCG* ST-associated genes (but not *CSH1* and *SDC1*) were induced (**Fig. 4H and fig. S10**). These results suggested that ST-like cells generated from HG-blastoids were partially functionalized as STs. Moreover, the secretion of hCG (a chemical secreted from trophoblast tissues, detected during normal pregnancy) was detected in the culture medium 4 days after *in vitro* implantation of HG-blastoids (**Fig. 4I**), suggesting that trophoblast-like cells appeared in attached HG-blastoids like that of natural human blastocysts.

Recently, the International Society for Stem Cell Research (ISSCR) updated its guidelines for stem cell research and clinical translation (*38*). The ISSCR recommends that research with *in vitro* embryo models containing the epiblast and extraembryonic endoderm, covered by trophectoderm-like cells (e.g., blastoid), would not be permitted in *in vitro* culture beyond the appearance of the primitive streak. Therefore, we measured the expression of *TBXT*, *EOMES*, or *MIXL1* as primitive streak markers (*39*, *40*) in the attached HG-blastoids in a dish for 4 days, and, we confirmed that HG-blastoids did not express these markers, as confirmed by quantitative RT-PCR (**fig. S11**).

Discussion

We established a simple method to generate blastoids from human primed embryonic stem cells by applying the proper physical environment with hydrogels (HG) to mimic that of natural human blastocysts. The obtained HG-blastoids showed similar patterns of cellular distribution (**Fig. 1**), molecular expression signatures (**Fig. 2**), and the capability to provide naive/primed PSCs and TSCs (**Fig. 3**), as natural human blastocysts. Moreover, they demonstrated implantation capability *in vitro* (**Fig. 4**). These capabilities illustrate its potential as a powerful tool for studying human early embryonic developmental processes *in vitro* (*16*, *41*).

To generate human blastoids from primed hESCs, we used a HG capable of mimicking the physical extracellular environment. A natural human blastocyst has a ZP glycoprotein layer, which functions as the selection layer for sperm and immunocontraception. The biochemical and physical properties of the ZP layer are well known (*42–46*). Particularly, it is known that the physical properties of the ZP layer change after fertilization, with zona hardening critical for preventing polyspermic penetration (*43*). The HG in this study showed 0.15 ± 0.04 kPa of Young's modulus (**fig. S1 and table S1**), which is softer than the reported Young's modulus of a natural ZP layer (ca. 10 - 40 kPa) (*19*, *44–46*). When we applied 2.01 ± 0.10 kPa for blastoid formation of primed hESCs, no blastoids were obtained. Without the HG, hESC aggregates in the cell culture medium with 10 % (v/v) serum did not form blastocyst-like structures but rather formed embryoid bodies (EB) that contained three germ layers (ectoderm, mesoderm, and endoderm). This method is traditionally used to induce the differentiation of hPSCs into the desired tissue cells; however, the generated EBs have random cell distributions. When we applied the HG with 10 % (v/v) serum, the outer layer of the hPSC aggregates received the biochemical and physical stimuli, inducing differentiation to the trophectoderm lineage. The

cells inside the hPSC aggregates, however, did not receive these stimuli and maintained their EPI phenotype. Therefore, although the HG used for blastoid formation was softer than that of the ZP layer, such a physical environment is critical for obtaining blastoids from primed hPSCs. Since the higher stiffness of the ZP layer mainly prevents massive sperm penetration into an oocyte, it might not be necessary to generate blastoid formation. Such a layer could not adhere to cells in a blastocyst or blastoid because they could not maintain a blastocyst-like structure due to their migration. Therefore, extracellular matrix proteins or cell-adhesive polymers (e.g., poly-L-lysine) would not be suitable to generate blastoids. Conversely, non-adhesive polymers (e.g., agarose) support the formation of blastoids from primed hESCs.

In 2021, the number of studies on human blastoid generation increased, yet, the cell sources in these studies were quite diverse. Liu et al. (2021) showed that cells treated for reprogramming from fibroblasts to hiPSCs have a variety of cell types (e.g., EPI-, TE-, and PE-like cells), and have the ability to form blastoids (*13*). However, cellular heterogeneity during reprogramming is unpredictable and unregulatable, as the obtained blastoids showed more cellular components, which natural blastocysts at E5–E7 did not (**Fig. 2D and E**). Instead of using reprogrammed cells, other reports used naive hPSCs to obtain blastoids (*14*, *15*). As previously reported, the naive state is considered more undifferentiated than the primed state (*47*). Human PSCs were thought unable to differentiate into extraembryonic cell lineages (e.g., trophoblast stem cells for forming placenta). However, recent studies have shown that naive hPSCs can differentiate into these lineages by changing their culture conditions (*23*, *48*, *49*). Therefore, undifferentiated naive hPSCs were used to generate blastoids. Recent studies have shown that primed hPSCs can be converted to a naive state. However, naive hPSCs cultured in 5i/L/A show genomic instability during culturing due to the hypomethylated state of the genome (*17*, *18*). The culture conditions for naive hPSCs are still being optimized compared with those of primed hPSCs. To the best of our knowledge, human blastoids have not yet been generated from primed human PSCs. Although the underlying mechanism is still unclear, the presented approach is a promising approach to study the processes and mechanisms underlying the generation of human blastoids from primed hPSCs. Moreover, it is capable of producing naive/primed PSCs and TSCs. In mouse models, a recent study showed that primed mESCs to blastoids (*10*) could be a useful tool for elucidating the generation of blastoids from primed human ESCs.

Finally, the HG-blastoids were capable of undergoing an implantation process *in vitro*, showing the formation of a lumen-like pro-amniotic cavity, trophoblast tissues, and secretion of hCG, without expressing primitive streak markers (*TBXT*, *EOMES*, or *MIXL1*) (**fig. S11**). By using such blastoid models, we can recapitulate and study the early human embryo developmental process before the appearance of the primitive streak (*38*, *50*). Although the ISSCR updated the guidelines for human embryo models derived from stem cells, a discussion is needed on how we can achieve a good balance between the advancement of the fundamental understanding of human development and ethical concerns.

This method had some limitations that need to be addressed. Although we were able to generate HG-blastoids from primed hPSCs, the efficiency was still low (14.1 %) compared to that of other reported methods using naive hPSCs. We hypothesized that primed hPSCs could be partially converted to a naive state by the physical environment of the HG, and then undergo blastoid formation. Therefore, the conversion would be the rate-limiting step for blastoid formation. Additionally, selection methods for proper blastoids have not yet been well established. The selection methods and quality checks for the obtained blastoids were based on microscopic imaging to observe their morphologies. In particular, the methods used for quality checking were

originally established for blastocysts by *in vitro* fertilization (IVF), with no concerns regarding contamination of other types of cells. According to the scRNA-seq results, the reported blastoids, including HG-blastoids, contained impurities in the cells, which should not exist in a natural human blastocyst. Therefore, the selection methods for high-quality blastoids require microscopic imaging to observe not only blastocyst-like morphology, but also molecular markers for EPI-, TE-, and PE-like cells.

In conclusion, we established a simple and robust method for generating human HG-blastoids from naive hESCs treated with a physically tuned HG. We envision that this method could be further improved to develop clinically relevant and chemically defined conditions to understand the basis of early human embryonic development. This method could be extended to other species to understand the fundamentals of early embryonic development by comparing multiple species without using their embryos. Finally, it can be used for high-throughput screening in drug discovery for pregnancy failure and birth defects prevention.

References and Notes

1. J. Rossant, P. P. L. Tam, New Insights into Early Human Development: Lessons for Stem Cell Derivation and Differentiation. *Cell Stem Cell*. **20**, 18–28 (2017).
2. J. A. Thomson, J. Itskovitz-Eldor, S. S. Shapiro, M. A. Waknitz, J. J. Swiergiel, V. S. Marshall, J. M. Jones, Embryonic stem cell lines derived from human blastocysts. *Science.* **282**, 1145–7 (1998).
3. A. Simon, N. Laufer, Assessment and treatment of repeated implantation failure (RIF). *J. Assist. Reprod. Genet.* **29**, 1227–1239 (2012).
4. E. R. Norwitz, Defective implantation and placentation: laying the blueprint for pregnancy complications. *Reprod. Biomed. Online*. **13**, 591–599 (2006).
5. C. De Geyter, C. Wyns, C. Calhaz-Jorge, J. de Mouzon, A. P. Ferraretti, M. Kupka, A. Nyboe Andersen, K. G. Nygren, V. Goossens, 20 years of the European IVF-monitoring Consortium registry: what have we learned? A comparison with registries from two other regions. *Hum. Reprod.* **35**, 2832–2849 (2020).
6. K. Takahashi, S. Yamanaka, Induction of Pluripotent Stem Cells from Mouse Embryonic and Adult Fibroblast Cultures by Defined Factors. *Cell*. **126**, 663–676 (2006).
7. K. Takahashi, K. Tanabe, M. Ohnuki, M. Narita, T. Ichisaka, K. Tomoda, S. Yamanaka, Induction of Pluripotent Stem Cells from Adult Human Fibroblasts by Defined Factors. *Cell*. **131**, 861–872 (2007).
8. T. Boroviak, J. Nichols, Primate embryogenesis predicts the hallmarks of human naïve pluripotency. *Development*. **144**, 175–186 (2017).
9. T. Nakamura, I. Okamoto, K. Sasaki, Y. Yabuta, C. Iwatani, H. Tsuchiya, Y. Seita, S. Nakamura, T. Yamamoto, M. Saitou, A developmental coordinate of pluripotency among mice, monkeys and humans. *Nature*. **537**, 57–62 (2016).
10. C. Kime, H. Kiyonari, S. Ohtsuka, E. Kohbayashi, M. Asahi, S. Yamanaka, M. Takahashi, K. Tomoda, Induced 2C Expression and Implantation-Competent Blastocyst-like Cysts from Primed Pluripotent Stem Cells. *Stem Cell Reports*. **13**, 485–498 (2019).

11. N. C. Rivron, J. Frias-Aldeguer, E. J. Vrij, J.-C. Boisset, J. Korving, J. Vivié, R. K. Truckenmüller, A. van Oudenaarden, C. A. van Blitterswijk, N. Geijsen, Blastocyst-like structures generated solely from stem cells. *Nature*. **557**, 106–111 (2018).

12. B. Sozen, A. L. Cox, J. De Jonghe, M. Bao, F. Hollfelder, D. M. Glover, M. Zernicka-Goetz, Self-Organization of Mouse Stem Cells into an Extended Potential Blastoid. *Dev. Cell*. **51**, 698-712.e8 (2019).

13. X. Liu, J. P. Tan, J. Schröder, A. Aberkane, J. F. Ouyang, M. Mohenska, S. M. Lim, Y. B. Y. Sun, J. Chen, G. Sun, Y. Zhou, D. Poppe, R. Lister, A. T. Clark, O. J. L. Rackham, J. Zenker, J. M. Polo, Modelling human blastocysts by reprogramming fibroblasts into iBlastoids. *Nature*. **591**, 627–632 (2021).

14. A. Yanagida, D. Spindlow, J. Nichols, A. Dattani, A. Smith, G. Guo, Naive stem cell blastocyst model captures human embryo lineage segregation. *Cell Stem Cell*. **28**, 1016-1022.e4 (2021).

15. L. Yu, Y. Wei, J. Duan, D. A. Schmitz, M. Sakurai, L. Wang, K. Wang, S. Zhao, G. C. Hon, J. Wu, Blastocyst-like structures generated from human pluripotent stem cells. *Nature*. **591**, 620–626 (2021).

16. X. Wang, G. Hu, Human embryos in a dish – modeling early embryonic development with pluripotent stem cells. *Cell Regen.* **11**, 4 (2022).

17. T. W. Theunissen, M. Friedli, Y. He, E. Planet, R. C. O'Neil, S. Markoulaki, J. Pontis, H. Wang, A. Iouranova, M. Imbeault, J. Duc, M. A. Cohen, K. J. Wert, R. Castanon, Z. Zhang, Y. Huang, J. R. Nery, J. Drotar, T. Lungjangwa, D. Trono, J. R. Ecker, R. Jaenisch, Molecular Criteria for Defining the Naive Human Pluripotent State. *Cell Stem Cell*. **19**, 502–515 (2016).

18. W. A. Pastor, D. Chen, W. Liu, R. Kim, A. Sahakyan, A. Lukianchikov, K. Plath, S. E. Jacobsen, A. T. Clark, Naive Human Pluripotent Cells Feature a Methylation Landscape Devoid of Blastocyst or Germline Memory. *Cell Stem Cell*. **18**, 323–329 (2016).

19. Y. Murayama, M. Yoshida, J. Mizuno, H. Nakamura, S. Inoue, Y. Watanabe, K. Akaishi, H. Inui, C. E. Constantinou, S. Omata, Elasticity Measurement of Zona Pellucida Using a Micro Tactile Sensor to Evaluate Embryo Quality. *J. Mamm. Ova Res.* **25**, 8–16 (2008).

20. P.-H. Chang, H.-M. Chao, E. Chern, S. Hsu, Chitosan 3D cell culture system promotes naïve-like features of human induced pluripotent stem cells: A novel tool to sustain pluripotency and facilitate differentiation. *Biomaterials*. **268**, 120575 (2021).

21. K. Kamei, Y. Koyama, Y. Tokunaga, Y. Mashimo, M. Yoshioka, C. Fockenberg, R. Mosbergen, O. Korn, C. Wells, Y. Chen, Characterization of Phenotypic and Transcriptional Differences in Human Pluripotent Stem Cells under 2D and 3D Culture Conditions. *Adv. Healthc. Mater.* **5**, 2951–2958 (2016).

22. K. Kamei, Y. Mashimo, Y. Koyama, C. Fockenberg, M. Nakashima, M. Nakajima, J. Li, Y. Chen, 3D printing of soft lithography mold for rapid production of polydimethylsiloxane-based microfluidic devices for cell stimulation with concentration gradients. *Biomed. Microdevices*. **17**, 36 (2015).

23. J. Kojima, A. Fukuda, H. Taira, T. Kawasaki, H. Ito, N. Kuji, K. Isaka, A. Umezawa, H. Akutsu, Efficient production of trophoblast lineage cells from human induced pluripotent stem cells. *Lab. Investig.* **97**, 1188–1200 (2017).

24. H. Kumagai, H. Suemori, M. Uesugi, N. Nakatsuji, E. Kawase, Identification of small molecules that promote human embryonic stem cell self-renewal. *Biochem. Biophys. Res. Commun.* **434**, 710–716 (2013).

25. T. E. Ludwig, M. E. Levenstein, J. M. Jones, W. T. Berggren, E. R. Mitchen, J. L. Frane, L. J. Crandall, C. A. Daigh, K. R. Conard, M. S. Piekarczyk, R. A. Llanas, J. A. Thomson, Derivation of human embryonic stem cells in defined conditions. *Nat. Biotechnol.* **24**, 185–187 (2006).

26. T. E. Ludwig, V. Bergendahl, M. E. Levenstein, J. Yu, M. D. Probasco, J. A. Thomson, Feeder-independent culture of human embryonic stem cells. *Nat. Methods*. **3**, 637–646 (2006).

27. M. D. Ungrin, C. Joshi, A. Nica, C. Bauwens, P. W. Zandstra, Reproducible, Ultra High-Throughput Formation of Multicellular Organization from Single Cell Suspension-Derived Human Embryonic Stem Cell Aggregates. *PLoS One*. **3**, e1565 (2008).

28. C. L. Bauwens, R. Peerani, S. Niebruegge, K. A. Woodhouse, E. Kumacheva, M. Husain, P. W. Zandstra, Control of Human Embryonic Stem Cell Colony and Aggregate Size Heterogeneity Influences Differentiation Trajectories. *Stem Cells*. **26**, 2300–2310 (2008).

29. K. Watanabe, M. Ueno, D. Kamiya, A. Nishiyama, M. Matsumura, T. Wataya, J. B. Takahashi, S. Nishikawa, S. Nishikawa, K. Muguruma, Y. Sasai, A ROCK inhibitor permits survival of dissociated human embryonic stem cells. *Nat. Biotechnol.* **25**, 681–686 (2007).

30. Y. Hao, S. Hao, E. Andersen-Nissen, W. M. Mauck, S. Zheng, A. Butler, M. J. Lee, A. J. Wilk, C. Darby, M. Zager, P. Hoffman, M. Stoeckius, E. Papalexi, E. P. Mimitou, J. Jain, A. Srivastava, T. Stuart, L. M. Fleming, B. Yeung, A. J. Rogers, J. M. McElrath, C. A. Blish, R. Gottardo, P. Smibert, R. Satija, Integrated analysis of multimodal single-cell data. *Cell*. **184**, 3573-3587.e29 (2021).

31. R. Satija, J. A. Farrell, D. Gennert, A. F. Schier, A. Regev, Spatial reconstruction of single-cell gene expression data. *Nat. Biotechnol.* **33**, 495–502 (2015).

32. S. Petropoulos, D. Edsgärd, B. Reinius, Q. Deng, S. P. Panula, S. Codeluppi, A. Plaza Reyes, S. Linnarsson, R. Sandberg, F. Lanner, Single-Cell RNA-Seq Reveals Lineage and X Chromosome Dynamics in Human Preimplantation Embryos. *Cell*. **165**, 1012–1026 (2016).

33. H. Okae, H. Toh, T. Sato, H. Hiura, S. Takahashi, K. Shirane, Y. Kabayama, M. Suyama, H. Sasaki, T. Arima, Derivation of Human Trophoblast Stem Cells. *Cell Stem Cell*. **22**, 50-63.e6 (2018).

34. M. Rostovskaya, G. G. Stirparo, A. Smith, Capacitation of human naïve pluripotent stem cells for multi-lineage differentiation. *Development*. **146** (2019), doi:10.1242/dev.172916.

35. M. N. Shahbazi, A. Jedrusik, S. Vuoristo, G. Recher, A. Hupalowska, V. Bolton, N. M. E. Fogarty, A. Campbell, L. G. Devito, D. Ilic, Y. Khalaf, K. K. Niakan, S. Fishel, M.

Zernicka-Goetz, Self-organization of the human embryo in the absence of maternal tissues. *Nat. Cell Biol.* **18**, 700–708 (2016).

36. S. Haider, G. Meinhardt, L. Saleh, V. Kunihs, M. Gamperl, U. Kaindl, A. Ellinger, T. R. Burkard, C. Fiala, J. Pollheimer, S. Mendjan, P. A. Latos, M. Knöfler, Self-Renewing Trophoblast Organoids Recapitulate the Developmental Program of the Early Human Placenta. *Stem Cell Reports*. **11**, 537–551 (2018).

37. Y. Li, M. Moretto-Zita, F. Soncin, A. Wakeland, L. Wolfe, S. Leon-Garcia, R. Pandian, D. Pizzo, L. Cui, K. Nazor, J. F. Loring, C. P. Crum, L. C. Laurent, M. M. Parast, BMP4-directed trophoblast differentiation of human embryonic stem cells is mediated through a ΔNp63+ cytotrophoblast stem cell state. *Development*. **140**, 3965–3976 (2013).

38. I. Hyun, M. Munsie, M. F. Pera, N. C. Rivron, J. Rossant, Toward Guidelines for Research on Human Embryo Models Formed from Stem Cells. *Stem Cell Reports*. **14**, 169–174 (2020).

39. L. Xiang, Y. Yin, Y. Zheng, Y. Ma, Y. Li, Z. Zhao, J. Guo, Z. Ai, Y. Niu, K. Duan, J. He, S. Ren, D. Wu, Y. Bai, Z. Shang, X. Dai, W. Ji, T. Li, A developmental landscape of 3D-cultured human pre-gastrulation embryos. *Nature*. **577**, 537–542 (2020).

40. R. C. V. Tyser, E. Mahammadov, S. Nakanoh, L. Vallier, A. Scialdone, S. Srinivas, A spatially resolved single cell atlas of human gastrulation. *bioRxiv* (2020), doi:10.1101/2020.07.21.213512.

41. N. Moris, C. Alev, M. Pera, A. Martinez Arias, Biomedical and societal impacts of in vitro embryo models of mammalian development. *Stem Cell Reports*. **16**, 1021–1030 (2021).

42. S. Oehninger, Biochemical and functional characterization of the human zona pellucida. *Reprod. Biomed. Online*. **7**, 641–648 (2003).

43. Q.-Y. Sun, Cellular and molecular mechanisms leading to cortical reaction and polyspermy block in mammalian eggs. *Microsc. Res. Tech.* **61**, 342–348 (2003).

44. E. Priel, T. Priel, I. Szaingurten-Solodkin, T. Wainstock, Y. Perets, A. Zeadna, A. Harlev, E. Lunenfeld, E. Levitas, I. Har-Vardi, Zona pellucida shear modulus, a possible novel non-invasive method to assist in embryo selection during in-vitro fertilization treatment. *Sci. Rep.* **10**, 14066 (2020).

45. M. Khalilian, M. Navidbakhsh, M. R. Valojerdi, M. Chizari, P. E. Yazdi, Estimating Young's modulus of zona pellucida by micropipette aspiration in combination with theoretical models of ovum. *J. R. Soc. Interface*. **7**, 687–694 (2010).

46. K. Leonavicius, C. Royer, C. Preece, B. Davies, J. S. Biggins, S. Srinivas, Mechanics of mouse blastocyst hatching revealed by a hydrogel-based microdeformation assay. *Proc. Natl. Acad. Sci.* **115**, 10375–10380 (2018).

47. M. F. Pera, J. Rossant, The exploration of pluripotency space: Charting cell state transitions in peri-implantation development. *Cell Stem Cell*. **28**, 1896–1906 (2021).

48. C. Dong, M. Beltcheva, P. Gontarz, B. Zhang, P. Popli, L. A. Fischer, S. A. Khan, K. Park, E.-J. Yoon, X. Xing, R. Kommagani, T. Wang, L. Solnica-Krezel, T. W. Theunissen, Derivation of trophoblast stem cells from naïve human pluripotent stem cells. *Elife*. **9**, 1–26 (2020).

49. G. Guo, G. G. Stirparo, S. E. Strawbridge, D. Spindlow, J. Yang, J. Clarke, A. Dattani, A. Yanagida, M. A. Li, S. Myers, B. N. Özel, J. Nichols, A. Smith, Human naive epiblast cells possess unrestricted lineage potential. *Cell Stem Cell*. **28**, 1040-1056.e6 (2021).

50. T. Sawai, G. Okui, K. Akatsuka, T. Minakawa, Promises and rules. *EMBO Rep.* **22**, 1–3 (2021).

Acknowledgments: We thank Kaho Takamuro and Ayumi Kikkawa for their technical assistance. We thank Dr. Kouichi Hasegawa, Dr. Dan Ohtan Wang, Dr. Tomonori Nakamura and Prof. Michinori Saito for critical discussion. The authors thank to iCeMS Analysis Center to access the advanced microscopy and analytical instruments. The authors thank to Dr. Takefumi Kondo to carry out RNA sequencing. The WPI-iCeMS is supported by the World Premier International Research Centre Initiative (WPI), MEXT, Japan.

Funding:

Japan Society for the Promotion of Science 17H02083, 21H01728 (KK)

Author contributions:

Conceptualization: SI, XW, KK

Methodology: SI, XW, ST, AY, MT, KK

Investigation: SI, XW, ST, AY, KMZ, KS, KY, MT, KK

Visualization: SI, XW, AY, KMZ, KK

Funding acquisition: KK

Project administration: KK

Supervision: KK

Writing – original draft: SI, XW, KK

Writing – review & editing: SI, XW, KK

Competing interests: Kyoto University (X.W., S.T., and K.K.) filed a patent application based on the research presented herein (WO2021/079992A1). The rest of the authors declare no competing interests.

Data and materials availability: All data, code, and materials used in the analysis must be available in some form to any researcher for purposes of reproducing or extending the analysis. Include a note explaining any restrictions on materials, such as materials transfer agreements (MTAs). Note accession numbers to any data relating to the paper and deposited in a public database; include a brief description of the data set or model with the number. If all data are in the paper and supplementary materials, include the sentence "All data are available in the main text or the supplementary materials."

Supplementary Materials

Materials and Methods

Supplementary Text

Figs. S1 to S11

Tables S1 to S3

References (*1*–*16*)

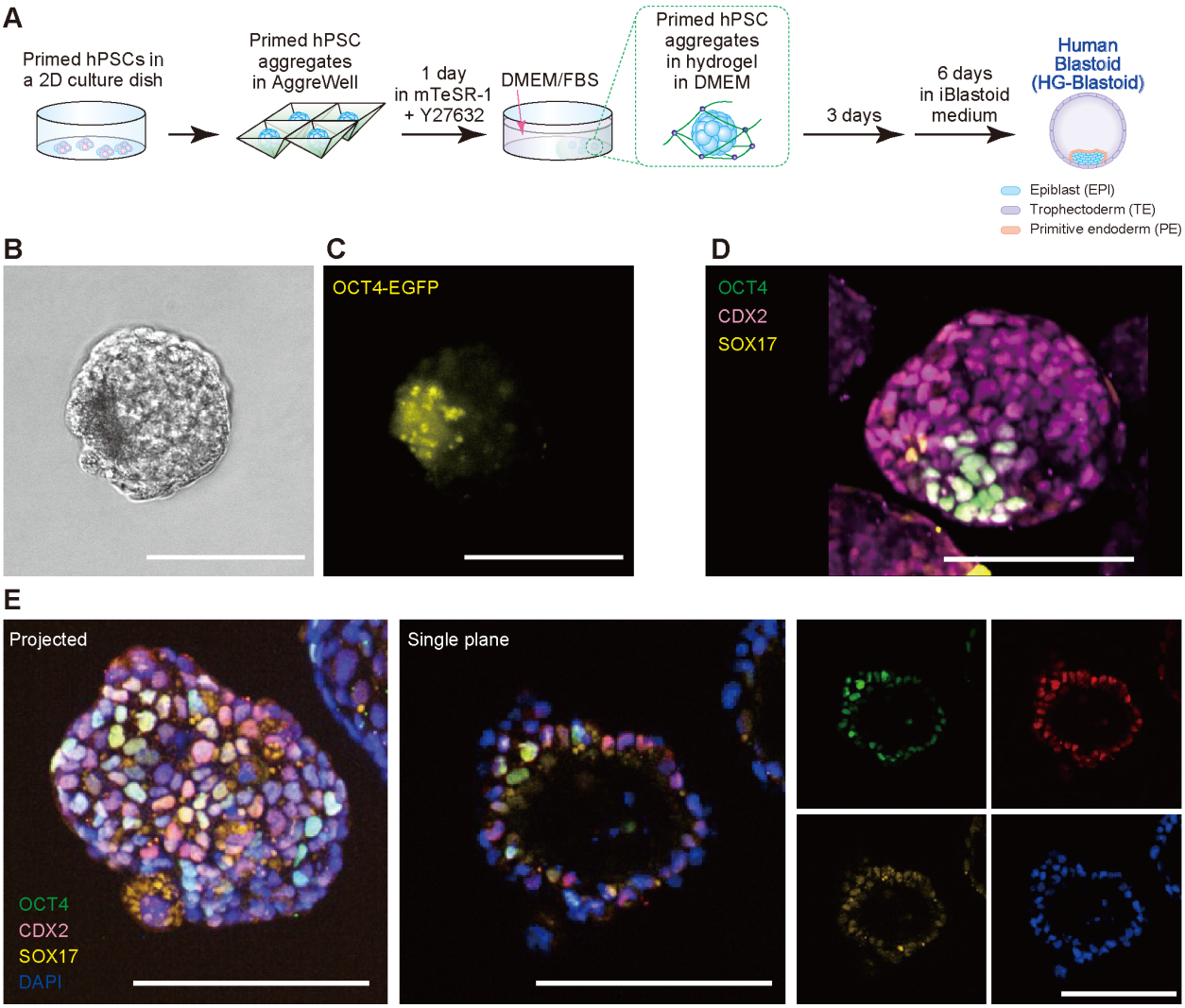

Fig. 1. The principle behind generating blastoids from human primed pluripotent stem cells (hPSCs). (**A**) A schematic showing the experimental process for generating HG-blastoids from primed hPSCs. TB, trophoblasts; ICM, inner cell mass; PE, primitive endoderm. Phase-contrast (**B**) and fluorescent (**C**) micrographs of an HG-blastoid derived from K1-OCT4-eGFP cells. (**D, E**) Whole-mount immunocytochemistry micrographs for the observation of typical markers of epiblast (OCT4), trophectoderm (CDX2), and primitive endoderm (SOX17) in HG-blastoids. DAPI was used to stain nuclei in images **E**. Scale bars represent 100 μm.

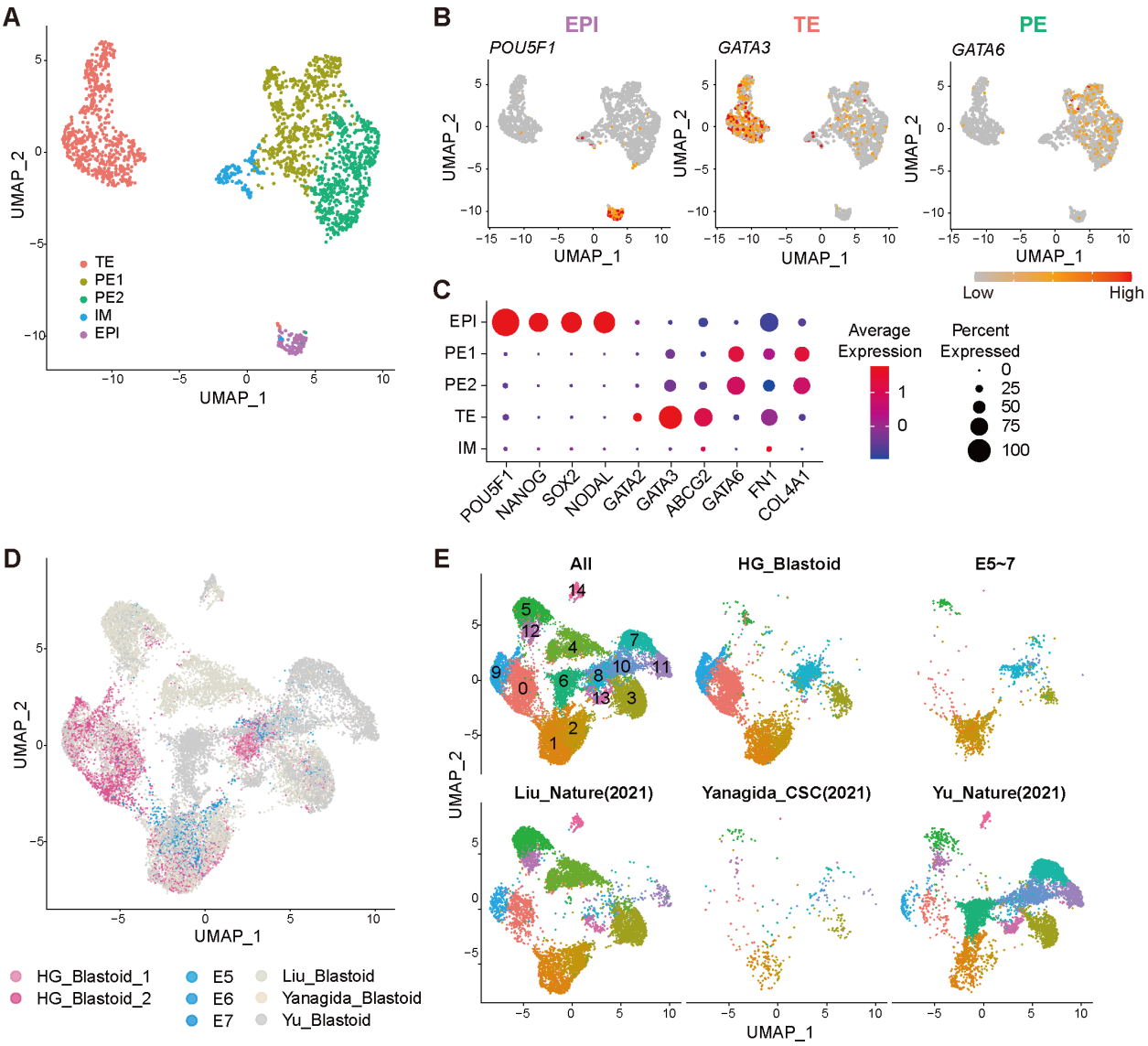

Fig. 2. Single-cell transcriptomic analyses of HG-blastoids. (A) UMAPs of the 2,072 cells in the HG-blastoid sc-RNA-seq library. (**B**) Expression of EPI (*POU5F1*), TE (*GATA3*), and PE (*GATA6*) marker genes. (**C**) A dot plot showing the expression of marker genes for EPI (*POU5F1, NANOG*, *SOX2*, and *NODAL*), TE (*GATA2*, *GATA3*, and *ABCG2*), and PE (*GATA6*, *FN1*, and *COL4A1*). Dot size and color (blue to red) represent the percentage of cells with the gene expression and averaged expression values. (**D-E**) Integrated and split UMAPs to show integrated scRNA-seq data sets consisting of data from HG-blastoids, human E5-E7 blastocysts (*32*), and published other blastoids (Yu_Nature [2021] (*15*), Liu_Nature [2021] (*13*), Yanagida_CSC [2021] (*14*)).

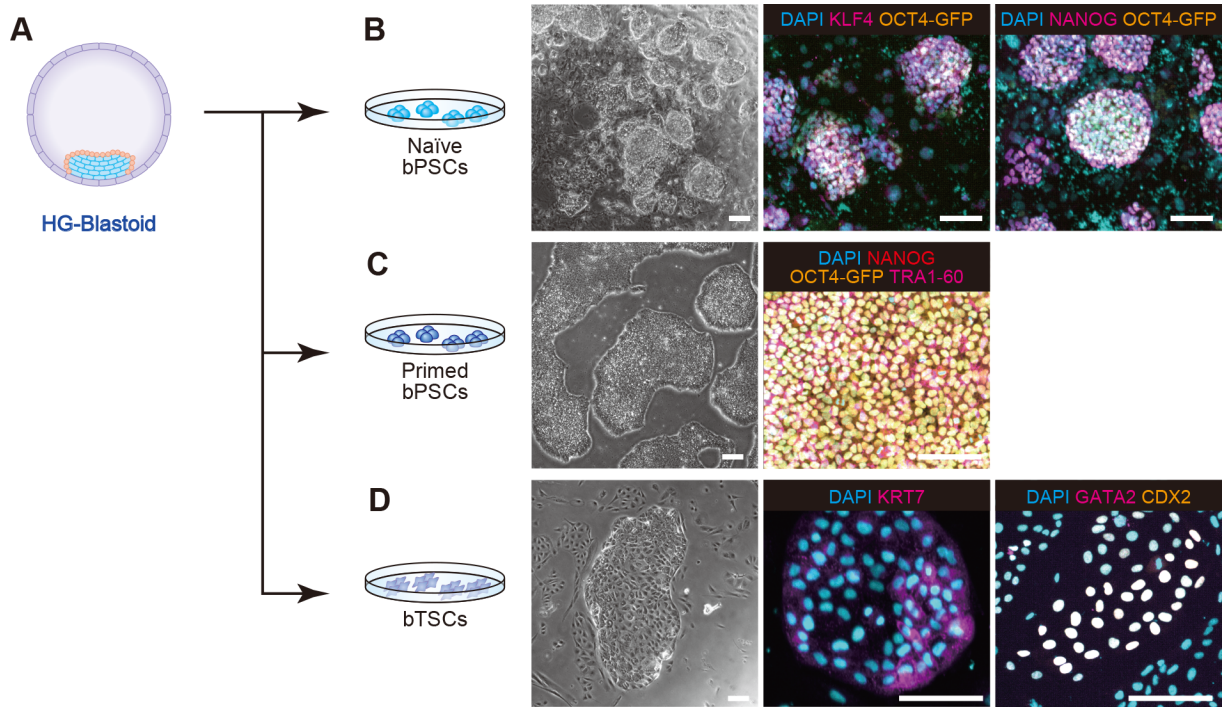

Fig. 3. Derivation of stem cells from HG-blastoids. (A) Blastocysts provide three kinds of stem cells, including naive/primed pluripotent stem cells (bPSCs) and trophoblast stem cells (bTSCs). **(B-D)** Phase-contrast and fluorescent micrographs of immunocytochemistry of naive bPSC visualized by KLF4, NANOG, and OCT4-eGFP **(B)**, primed bPSCs visualized by NANOG, TRA1-60, and OCT4-eGFP **(C)**, and bTSCs visualized by GATA2 and CDX2 **(D)**. DAPI was used to stain nuclei. Scale bars represent 100 μm.

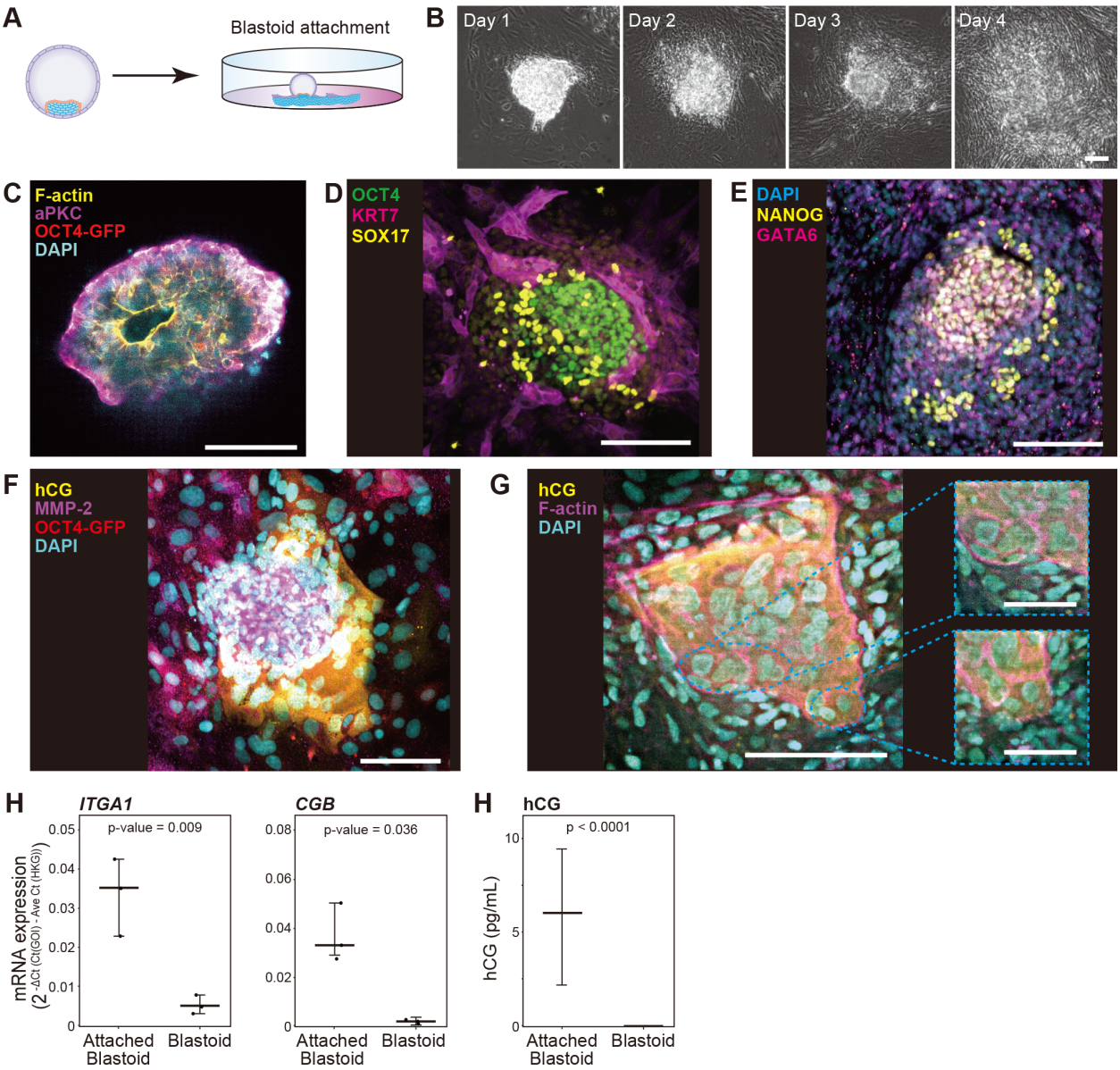

Fig. 4. *In vitro* implantation assay for HG-blastoids. (A) A schematic showing the *in vitro* implantation assay, whereby HG-blastoids were seeded onto the GelTrex-coated cell culture dish. **(B)** Micrographs of HG-blastoids attached to the dish. **(C-F)** Fluorescent micrographs of attached HG-blastoids, 4 days after *in vitro* implantation, immunostained with the following: **(C)** F-actin, OCT4, and aPKC; **(D)** OCT4, SOX17, and KRT7, to investigate the distribution of EPI-, PE- and TE-like cells, respectively; **(E)** NANOG and GATA6; **(F)** hCG and MMP2 (markers of extravillous cytotrophoblasts [EVTs] and syncytiotrophoblasts [STs], respectively); **(G)** hCG and F-actin. OCT4-GFP represents eGFP expression driven by the *OCT4* promoter. DAPI was used to stain nuclei in images **C**, **E**, **F** and **G**. Scale bars represent 100 µm, except scale bars in images **G** with dashed light blue squares represent 50 µm. **(H)** Quantitative RT-PCR analysis of gene expression associated with EVTs (e.g., *ITGA1*) and STs (*CGB*; also known as hCG). n = 3. **(I)** Quantification of hCG secreted from HG-blastoids and attached HG-blastoids. n = 3.